REPORT

NEAR-FIELD OPTICAL THERMOMETRY

Kenneth E. Goodson and Mehdi Asheghi
Mechanical Engineering Department, Stanford University, Stanford, California, USA

Far-field optical thermometry techniques have spatial resolution limited by diffraction to the order of the radiation wavelength. We report progress on near-field optical thermometry (NFOT) that targets spatial resolution better than 50 nm. A tapered, single-mode optical fiber scans nanometers above electronic microstructures, which are heated using transient electrical currents. The fiber tip releases about 1 nW of radiation power from a steady probe laser, and the reflected radiation is used to measure the local temperature. Simultaneous electrical resistance thermometry is used to estimate the relative importance of temperature-dependent optical properties of the sample and thermal expansion of the sample and tip. This work provides guidance for implementing other NFOT techniques using radiation transmission and infrared emission.

The resolution available for the optical characterization of surfaces was revolutionized by near-field scanning optical microscopy (NSOM) [1–7]. NSOM technology overcomes the diffraction limited spatial resolution of conventional far-field techniques by delivering or capturing radiation through an optical probe, such as a tapered, metal-coated optical fiber [3, 4, 6] or a hollowed tip at the end of a cantilever [1, 2, 5], which is scanned nanometers above the sample surface. Radiation interacts with a surface region of diameter comparable to that of the probe optical orifice, which can be smaller than 50 nm. Scanning the probe across the sample surface requires control of the tip–surface separation using atomic-scale normal or shear forces, in a manner similar to that used by the atomic force microscope (AFM). NSOM technology has been used for the formation and detection of ultrasmall magnetooptic domains [7], the spatial mapping of radiation

Accepted 7 March 1997.

The progress described here owes much to technical discussions with Olaf W. Käding (now with TEMIC) and Y. Sungtaeh Ju of Stanford University. Professor L. Balk from the University of Wuppertal, Germany provided helpful comments. The interconnect sample was provided by Intel Corporation and the SOI calibration structure was fabricated by Y. K. Leung and S. S. Wong of Stanford University. The NSOM in this study was obtained through support from ONR and Topometrix, Inc. Kenneth E. Goodson warmly appreciates the support of the ONR Young Investigator Program, the NSF CAREER Program, NSF grant CTS-9622178, and a Hewlett-Packard Terman Fellowship. Mehdi Asheghi appreciates support from SRC through contract 97-SJ-461.

This work was presented at the 1996 U.S.–Japan Joint Meeting on Molecular and Microscale Transport Phenomena, Santa Barbara, California, 8–10 August 1996.

Address correspondence to Prof. Kenneth E. Goodson, Mechanical Engineering Department, Stanford University, Stanford, CA 94305-3030, USA. E-mail: goodson@ stokes.stanford.edu

Microscale Thermophysical Engineering, 1:225–235, 1997

1089-3954/97 $12.00 + .00

NOMENCLATURE

D	diameter of radiation orifice in the metal coating at end of fiber tip, m	T	temperature, K
e	emissive power, W/m^2	T_s	sample surface temperature, K
f	heating frequency, Hz	T_t	fiber tip temperature, K
n	complex refractive index	δ	separation between the fiber tip and the sample surface, m
P	radiation power, W		

emission from semiconductor lasers [6], and the fluorescence imaging of living cells [4]. We report here our progress on using the NSOM for mapping temperatures at surfaces.

There have been many studies on surface thermometry with high spatial and temporal resolution [8]. The most accurate thermometry techniques use the temperature dependence of the electrical properties of bridges or junctions microfabricated on the surface of a sample [9, 10]. Although these techniques yield accurate local temperature data, they do not provide a temperature distribution and often require extensive sample preparation. Scanning thermal microscopy (SThM) uses a thermocouple junction at the tip of an AFM cantilever to map temperature with resolution better than 100 nm [11, 12]. This approach has proven excellent for mapping near-steady temperature distributions in transistors and laser diodes with the highest available spatial resolution. The disadvantage of electrical thermometry techniques, including SThM, is that electrical capacitance and voltage reflection effects dramatically complicate measurements performed with frequencies above a few hundred kilohertz. The fastest thermometry techniques use radiation–surface interactions. Laser reflectance thermometry was demonstrated with high temporal resolution on transistors [13] and interconnects [14]. Other optical thermometry techniques detect thermally induced surface displacement [15, 16] and temperature-dependent photon–phonon scattering [17, 18]. Since these optical techniques have previously been applied only in the far field, there is considerable motivation for the present feasibility study on near-field optical thermometry.

EXPERIMENTAL APPARATUS AND PROCEDURE

Because several different optical probing methods are available, a brief discussion is warranted here of their relative merits for thermometry. Most samples of practical interest for thermometry are opaque, such that the probe must allow reflected light to be distinguished from light not interacting with the surface. This is best achieved using a tapered optical fiber coated with an opaque metal layer that has an orifice at the tip [3, 4, 6]. The coating forces all light escaping from the fiber, which can be collected using a far-field objective, to interact with the surface. A straight optical fiber [3, 4] offers the further advantage that it preserves the polarization state of transmitted radiation, which allows radiation reflected back *within* the fiber to be routed to a detector using a polarizing beam splitter. However, straight optical-fiber probes have the important disadvantage that the tip–surface shear force, rather than the more sensitive normal force used for

conventional AFM, is used for controlling the tip–surface separation. One promising alternative is a bent optical fiber [6], which uses the normal force but does not preserve the radiation polarization state. Another alternative is an AFM cantilever with a hollowed tip [5], which also allows precise control of the tip–surface separation and can, in principle, preserve the radiation polarization state. However, a hollowed AFM cantilever tip is not well suited for reflection-mode NSOM, because radiation reflected by the cantilever overwhelms that reflected by the sample. There is no probing technique that is clearly best for thermometry.

The present study employs a straight, metal-coated optical fiber in the facility shown in Figure 1. The apparatus integrates a near-field scanning optical microscope with a voltage supply and chip mount that allows electrical currents to be sustained in the sample. About 3 mW of radiation from an air-cooled argon-ion laser is coupled into the optical fiber, whose end tapers to a diameter near 200 nm. Less than 10 nW escapes from the end of the taper through the orifice in the aluminum coating of diameter $D \cong 50$ nm. Radiation can be collected at a photomultiplier tube (PMT) using one of two far-field optical paths, which capture reflected and transmitted light, respectively. In addition, the apparatus in Figure 1 allows radiation reflected within the fiber to be routed to a photodiode by a quarter-wave plate and a polarizing beam splitter. In theory, thermometry can be performed using the impact of temperature changes on the collected radiation power along each of these three paths, as suggested by Table 1. The collected radiation for each path depends on the optical constants of the sample, which vary with temperature. This dependence is the principle behind far-field laser re-

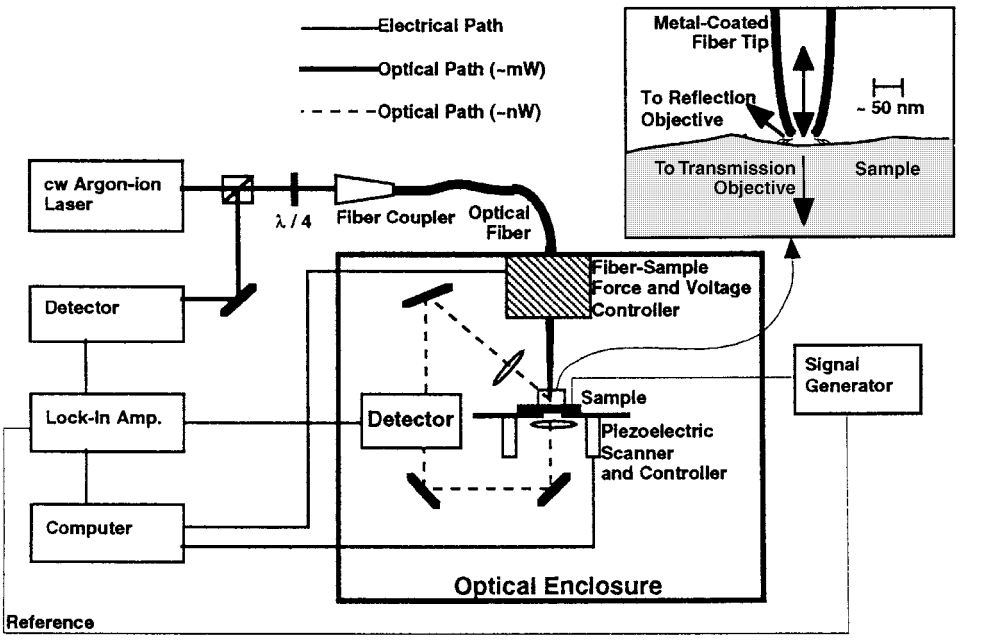

Figure 1. Schematic of the experimental apparatus and the tip–surface interaction region.

Table 1. Summary of near-field optical thermometry techniques proposed here

Near-field thermometry technique	Radiation source	Collection path	Comments
1. Laser reflectance, far-field collection	Probe laser through optical fiber	Far-field objective above sample	Data provided in this article in Figures 2 and 3. Resolution impaired somewhat by optical path around fiber tip.
2. Laser reflectance, fiber collection	Probe laser through optical fiber	Optical fiber, $\lambda/4$ plate, beam splitter	Radiation reflected from surface may prove impossible to extract from radiation reflected within fiber.
3. Laser transmittance	Probe laser through optical fiber	Far-field objective beneath sample	Appropriate only for samples that are not opaque.
4. Infrared emission	Sample surface infrared emission	Infrared-transmitting optical fiber	Possibility for large sensitivity. Dramatic improvement over far-field resolution, which is comparable to 5 μm at room temperature.

Note: Data were obtained for this article using technique 1 only. The anticipated relative merits of the different techniques are discussed in the text.

flectance thermometry [13, 14]. The collected radiation may also vary with temperature due to thermal expansion of the probe tip and of the sample. The next section discusses these mechanisms in greater detail and provides data obtained using the first experimental approach in Table 1, i.e., radiation is collected within the optical enclosure using a far-field objective. Table 1 indicates the possibility of highly promising near-field infrared thermometry, not explored experimentally in this article, in which the probe laser is not used.

The present article explores transient thermometry in the frequency domain by suspending the fiber above microelectronic structures heated by sinusoidal bias currents. The lock-in amplifier in Figure 1 measures the amplitude and phase of the collected radiation intensity at the heating frequency f, which is twice the frequency of the bias current. The calibration of the temperature amplitude corresponding to a given radiation amplitude is performed using a two-step procedure. First, the transient NFOT data are taken above a calibration bridge whose temperature can be assumed uniform and whose electrical resistance can be measured simultaneously. Second, the temperature dependence of the electrical resistance of the bridge is calibrated independently using a probe station and a thermal chuck. The calibration can be considered appropriate only for surfaces that closely resemble the calibration surface in roughness, purity, and stoichiometry.

An important feature of this measurement technology is the ability to scan the sample beneath the optical fiber. The samples are mounted on a piezoelectrically actuated x–y scanning stage, which allows the sample to be moved without altering the optical paths. Since the collected radiation power and its temperature dependence depend on the tip–surface separation, it is important that the

tip–surface separation remain constant during scanning. The tip–surface separation is controlled using the shear-force feedback mechanism, which uses a piezoelectric tube to oscillate the fiber tip laterally with frequency near 75 kHz and amplitude near 5 nm. The phase of the tip oscillations depends on the shear forces exerted on the probe by the sample, which vary strongly with the tip–sample separation. For practical measurements under atmospheric conditions, the forces imposed by a surface moisture layer are expected to dominate. The phase is monitored using radiation from another laser that passes around the probe tip and strikes a quad detector.

RESULTS AND DISCUSSION

Data interpretation must consider the thermophysical and geometric parameters influencing radiation interaction in the tip–surface region, which are summarized in Table 2. The variation of these parameters with the sample surface temperature makes surface thermometry possible. Since each of these parameters has different implications for the temporal and spatial resolution, it is important to study their relative importance. The complex refractive index of the sample surface influences the transmitted and reflected radiation power. The use of this parameter for thermometry is analogous to far-field laser reflectance techniques, which

Table 2. Temperature-dependent quantities that can influence the NFOT signal

Temperature-dependent quantity	Explanation	Associated temporal resolution limit	Associated spatial resolution limit
1. Sample surface complex refractive index, $\tilde{n}(T)$	Surface optical constants vary with temperature due to changing band structure and scattering rates.	Very brief, $\tilde{n}(T)$ is coupled with picosecond time scale to sample surface temperature changes.	$\sim D$; changes in $\tilde{n}(T)$ are relevant only near surface in region of diameter near D.
2. Sample surface emissive power, $e(T)$	Photon emission from surface increases rapidly with temp. Relevant only for proposed near-field infrared imaging.	Very brief; $e(T)$ is coupled with picosecond time scale to sample surface temperature changes.	$\sim D$; changes in $e(T)$ are relevant only near surface in region of diameter near D.
3. Fiber coating orifice diameter, $D(T)$	Fiber tip is heated by sample, causing thermal expansion to increase the orifice diameter.	$>$ 1 ns; heat must diffuse 5 nm normal to surface moisture layer into fiber.	$\sim D$; changes in D are dominated by conduction from local region at sample surface.
4. Separation between fiber tip and surface, $\delta(T)$	Transient thermal expansion of sample and tip reduce sample–tip separation.	$<$ 1 ns; governed by time to achieve thermomechanical equilibrium in sample.	Dictated by dimensions of region dominating thermal expansion. Tip expansion can also be important.

Note: Although each of these mechanisms provides a measure of the surface temperature near the probe–surface interaction region, mechanisms 1 and 2 provide the highest temporal and spatial resolution.

offer very high temporal resolution. The sensitivity in the near field may be enhanced by the excitation of surface plasmons [19]. If the fiber is significantly heated by conduction from the sample through a surface moisture layer, then the fiber optical throughput may be affected due to changes in its diameter, length, and material indices of refraction [20, 21]. The impact of the changing tip diameter may be the most important among these three mechanisms because conduction from the sample induces the largest temperature rise at the tip. Thermal expansion of the near-surface region in the sample diminishes the tip–surface separation δ, which influences the collected radiation power. The use of sample thermal expansion is analogous to far-field photothermal displacement techniques, which can offer very high temporal resolution.

It is possible to estimate the impact of these thermometry mechanisms on the phase of frequency-domain data using complex algebra. The phase and relative amplitude of radiation power oscillations is approximately

$$\frac{\tilde{P}_f}{P} \sim \left(\frac{1}{P} \frac{\partial P}{\partial \tilde{n}} \frac{\partial \tilde{n}}{\partial T_s} + \frac{1}{P} \frac{\partial P}{\partial \delta} \frac{\partial \delta}{\partial T_s} \right) \tilde{T}_{s,f} + \left(\frac{1}{P} \frac{\partial P}{\partial D} \frac{\partial D}{\partial T_t} + \frac{1}{P} \frac{\partial P}{\partial \delta} \frac{\partial \delta}{\partial T_t} \right) \tilde{T}_{t,f} \quad (1)$$

where P is the time-averaged power, T_s is the surface temperature, and T_t is the fiber tip temperature. The amplitude and phase of the power and temperature oscillations at the frequency f are represented using complex quantities and the subscript f. The second term in parentheses on the right of Eq. (1) neglects temperature variations in the heated fiber region. Prediction of the partial derivatives of P would require simulations of the electromagnetic energy transfer in the tip–surface region, which have been performed previously for two-dimensional isothermal geometries [22, 23] and are beyond the scope of the present study. The first term in the first pair of parentheses is analogous to the thermoreflectance coefficient for far-field photothermal microscopy, whose sign can be either positive or negative and depends on the optically interrogated materials. The second term in the first set of parentheses is expected to have negative sign because expansion of the sample reduces the separation and diminishes the radiation power reflected into the far field. This results in a 180° phase shift for its contribution to the complex power amplitude. The first and second terms in the second set of parentheses are expected to have positive and negative real values, respectively. A phase lag between the temperature of the tip and the surface temperature is expected to become important at high frequencies. These phases are used to interpret data from the calibration structure.

Calibration is demonstrated using the structure shown in Figure 2*a*, in which the temperature can be measured directly using a doped silicon electrical resistance thermometer. Heat is generated by a neighboring metallic interconnect. The structure does not sustain large spatial temperature gradients at the silicon dioxide surface due to the overlying silicon layer, which effectively conducts heat laterally above the buried silicon dioxide. To study the impact of tip–surface heat diffusion, data are obtained for two very different values of this separation. For the smaller value of δ, the tip is controlled using shear-force feedback at a separation of 5 ± 1 nm. This separation value is measured destructively by moving the fiber tip toward

the surface until it begins to scrape, which increases the radiation released by the fiber. For the larger value of δ, the tip–surface separation is about 3 μm and the feedback is not engaged. Figure 2*b* compares the phase of the detected oscillations in the collected radiation power for these two cases with the phase of the electrically measured thermistor temperature. The phase lag of the thermistor temperature with respect to the heating intensity approaches zero for low frequencies and increases with increasing frequency. The two sets of optical thermometry data agree reasonably well in the frequency range 8–50 kHz. This suggests that surface–tip heat diffusion, which must be absent for the case of the large separation, is not important for near-field measurements at high frequencies. At high frequencies, the qualitative agreement between the optical and thermistor data indicates that the temperature dependence of the tip–surface separation, for which these two data sets should differ by 180°, is not important. Equation (1) therefore suggests that the temperature dependence of the optical constants dominates the

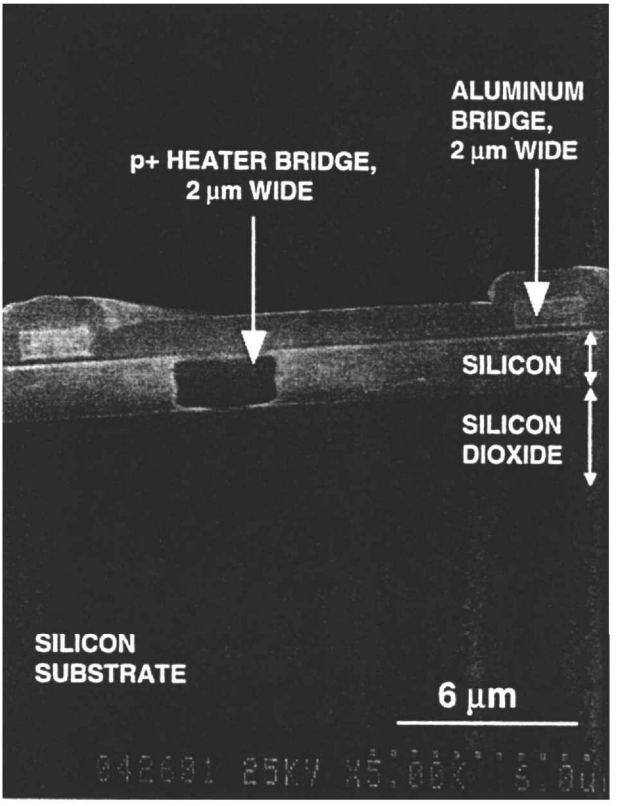

(*a*)

Figure 2. (*a*) Scanning electron micrograph of the calibration structure studied here, which is fabricated at the surface of a silicon-on-insulator substrate. A silicon layer containing a heavily doped bridge is sandwiched between two silicon dioxide layers.

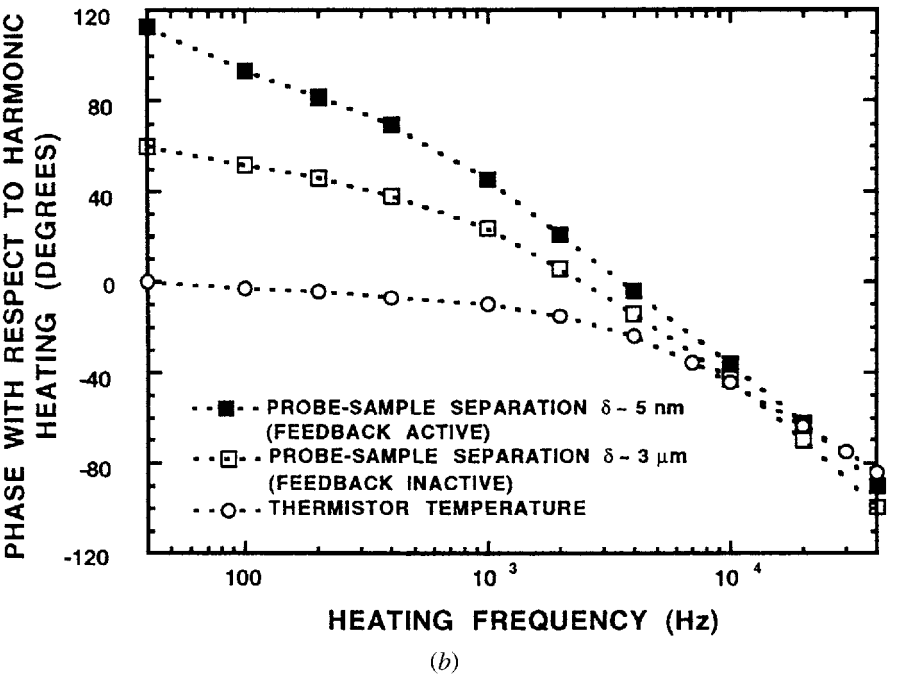

(*b*)

Figure 2. (*Continued*) (*b*) Phase of detected radiation power fluctuations and of the calibrated temperature.

measurement at high frequencies. Surface–tip heat diffusion and thermal expansion of the tip grow in importance at low frequencies, which may account for the disagreement between the optical and thermistor phase data below about 8 kHz. These two phenomena also grow in importance with decreasing tip–surface separation, which explains the disagreement of the two sets of optical data at these frequencies.

Figure 3 provides thermometry data for two adjacent aluminum interconnects at the surface of passivation in a VLSI test circuit. The interconnect on the right sustains a bias current at 1 kHz, resulting in heating at the frequency 2 kHz. The interconnect is cooled by thermal conduction to its contact pad, visible at the bottom of the image, which experiences little Joule heating due to its large cross section for the bias current. The temperature field along this conduction path is evident in the spatial distribution of the collected radiation power fluctuations, which decrease with decreasing separation from the contact pad and are consistent with far-field laser reflectance thermometry performed on a similar structure [14]. The interconnect on the left sustains no bias current and therefore has a much smaller temperature amplitude. The temperature in the contact pad is larger than that recorded in the unheated interconnect, because of conduction along the heated interconnect. The peak in temperature near the edge of the contact pad appears to be an artifact occurring when radiation must traverse the edge of the contact pad before reaching the far-field detector. More research is needed to

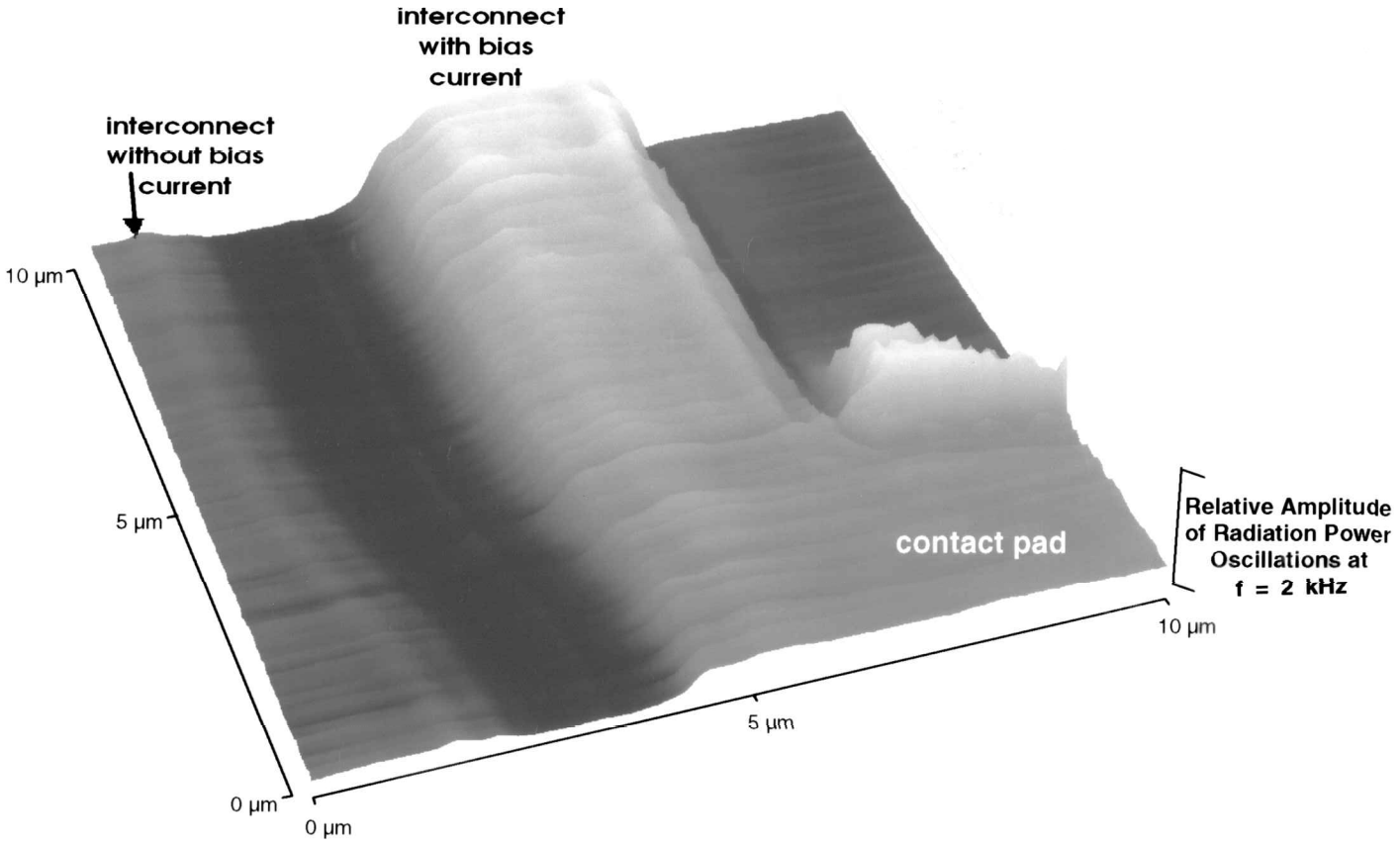

Figure 3. Relative amplitude of radiation power oscillations at the heating frequency of 2 kHz for a NFOT scan above two neighboring interconnects in the vicinity of a contact pad. The interconnect on the right sustains a bias current and 1 kHz and is cooled by conduction to the unheated, wider contact pad. The interconnect on the left does not sustain a bias current. The peak temperature amplitude in the interconnect on the right is approximately 50 K.

determine if this artifact results from the enhanced excitation of surface plasmons or from a locally heightened sensitivity to thermal expansion of the sample.

CONCLUDING REMARKS

This study shows that radiation collected using reflection-mode NSOM can be used to map temperature distributions at interconnect surfaces in VLSI circuits. The present work also shows that for transient measurements performed in the frequency domain, the phase of the collected radiation provides information about the mechanisms responsible for the thermometry. For the silicon/silicon dioxide calibration structure studied here, this approach strongly indicates that the optical signal above about 8 kHz is induced by the temperature-dependent optical properties of the sample rather than by thermal expansion of the fiber or the sample. Further studies are needed to determine the relative importance of these mechanisms for lower frequencies and for samples consisting of materials with larger thermal expansion coefficients. For measurements at time scales well below 1 μs, heat diffusion into the probe tip may be of minimal importance and the signal may be governed only by the temperature dependence of the sample optical properties and of the tip–surface separation. The careful use of and distinction between these two mechanisms promises to yield near-field thermometry techniques analogous to the well-established far-field laser reflectance and photothermal displacement methods. Additional work using the apparatus and phase analysis employed here aims to establish the feasibility of a near-field counterpart to highly sensitive infrared imaging, which promises to improve the spatial resolution of this technique by nearly two orders of magnitude.

REFERENCES

1. D. W. Pohl, W. Denk, and M. Lanz, Optical Stethoscopy: Image Recording with Resolution $\lambda/20$, *Appl. Phys. Lett.*, vol. 44, pp. 651–653, 1984.
2. U. Dürig, D. W. Pohl, and F. Rohner, Near-Field Optical-Scanning Microscopy, *J. Appl. Phys.*, vol. 59, pp. 3318–3327, 1986.
3. E. Betzig, J. K. Trautman, T. D. Harris, J. S. Weinder, and R. L. Kostelak, Breaking the Diffraction Barrier: Optical Microscopy on a Nanometric Scale, *Science*, vol. 251, pp. 1468–1470, 1991.
4. E. Betzig and J. K. Trautman, Near-Field Optics: Microscopy, Spectroscopy, and Surface Modification beyond the Diffraction Limit, *Science*, vol. 257, pp. 189–195.
5. M. Radmacher, P. E. Hillner, and P. K. Hansma, Scanning Nearfield Optical Microscope Using Microfabricated Probes, *Rev. Sci. Instrum.*, vol. 65, pp. 2737–2738, 1994.
6. U. Ben-Ami, N. Tessler, N. Ben-Ami, R. Nagar, G. Fish, K. Lieberman, G. Eisenstein, A. Lewis, J. M. Nielsen, and A. Moeller-Larsen, Near-Infrared Contact Mode Collection Near-Field Optical and Normal Force Microscopy of Modulated Multiple Quantum Well Lasers, *Appl. Phys. Lett.*, vol. 68, pp. 2237–2239, 1996.
7. E. Betzig, J. K. Trautman, R. Wolfe, E. M. Gyorgy, and P. L. Finn, Near-Field Magneto-Optics and High-Density Data Storage, *Appl. Phys. Lett.*, vol. 61, pp. 142–144, 1992.

8. K. E. Goodson, Y. S. Ju, and M. Asheghi, Thermal Phenomena in Semiconductor Devices and Interconnects, in C. L. Tien, A. Majumdar, and F. Gerner (eds.), *Microscale Energy Transport*, Taylor & Francis, Washington, DC, in press.
9. K. E. Goodson, M. I. Flik, L. T. Su, and D. A. Antoniadis, Prediction and Measurement of Temperature Fields in Silicon-on-Insulator Electronic Circuits, *ASME J. Heat Transfer*, vol. 117, pp. 574–581, 1995.
10. K. Banerjee, A. Amerasekera, and C. Hu, Characterization of VLSI Circuit Interconnect Heating and Failure under ESD Conditions, *Proc. Int. Reliability Physics Symp.*, pp. 237–245, 1996.
11. A. Majumdar, J. P. Carrejo, and J. Lai, Thermal Imaging Using the Atomic Force Microscope, *Appl. Phys. Lett.*, vol. 62, pp. 2501–2503, 1993.
12. A. Majumdar, J. Lai, M. Chandrachood, O. Nakabeppu, Y. Wu, and Z. Shi, Thermal Imaging by Atomic Force Microscopy Using Thermocouple Cantilever Probes, *Rev. Sci. Instrum.*, vol. 66, pp. 3584–3592, 1995.
13. Y. S. Ju, O. W. Käding, Y. K. Leung, S. S. Wong, and K. E. Goodson, Transient Thermal Mapping of SOI LDMOS Transistors, *Electron Device Lett.*, vol. 18, pp. 169–171, 1997.
14. Y. S. Ju and K. E. Goodson, Short-Timescale Thermometry and Reliability Studies on Interconnects, presented at the International Reliability Physics Symposium, Denver, Colorado, 8–10 April 1997, *IEEE Catalog No. 97 CH 35983*, pp. 320–324.
15. Y. Martin and H. K. Wickramasinghe, Study of Dynamic Current Distribution in Logic Circuits by Joule Displacement Microscopy, *Appl. Phys. Lett.*, vol. 50, pp. 167–168, 1987.
16. W. Claeys, S. Dilhaire, V. Quintard, J. P. Dom, and Y. Danto, Thermoreflectance Optical Test Probe for the Measurement of Current-Induced Temperature Changes in Microelectronic Components, *Reliability Eng. Int.*, vol. 9, pp. 303–308, 1993.
17. H. Brugger, Raman Spectroscopy for Characterization of Lazered Semiconductor Materials and Devices, in K. J. Lockwood and J. F. Young (eds.), *Light Scattering in Semiconductor Structures and Superlattices*, pp. 259–274, Plenum Press, New York.
18. R. Ostermeier, K. Brunner, G. Abstreiter, and W. Weber, Temperature Distribution in Si-MOSFET's Studied by Micro Raman Spectroscopy, *IEEE Trans. Electron Devices*, vol. 39, pp. 858–863, 1992.
19. S. Herminghaus and P. Leiderer, Surface Plasmon Enhanced Transient Thermoreflectance, *Appl. Phys.*, vol. A51, pp. 350–353, 1990.
20. D. I. Kavaldjiev, R. Toledo-Cros, and M. Vaez-Iravani, On the Heating of the Fiber Tip in a Near-Field Scanning Optical Microscope, *Appl. Phys. Lett.*, vol. 67, pp. 2771–2774, 1995.
21. B. I. Yakobson, A. LaRosa, H. D. Hallen, and M. A. Paesler, Thermal/Optical Effects in NSOM Probes, *Ultramicroscopy*, vol. 61, pp. 179–185, 1995.
22. L. Novotny, D. W. Pohl, and P. Regli, Near-Field, Far-Field and Imaging Properties of the 2D Aperture SNOM, *Ultramicroscopy*, vol. 57, pp. 180–188, 1995.
23. A. Castiaux, A. Dereux, J.-P. Vigneron, C. Girard, and O. J. F. Martin, Electromagnetic Fields in Two-Dimensional Models of Near-Field Optical Microscope Tips, *Ultramicroscopy*, vol. 60, pp. 1–9, 1995.